Competition between charge and bond waves in a Peierls-Hubbard model

1990 J. Phys.: Condens. Matter 2 3723

(http://iopscience.iop.org/0953-8984/2/16/003)

J. Phys.: Condens. Matter 2 (1990) 3723–3735. Printed in the UK

Competition between charge and bond waves in a Peierls–Hubbard model

Jaime Rössler† and David Gottlieb†‡

† Facultad de Ciencias, Universidad de Chile, Casilla 653, Santiago, Chile
‡ Centro de Física El Trauco, Fanor Velasco 41-D, Santiago, Chile

Received 1 September 1989, in final form 12 December 1989

Abstract. We study a one-dimensional extended Hubbard–Peierls model in the infinite intracell Coulomb repulsion limit, which is equivalent to a system of spinless electrons. We consider first- and second-neighbour Coulomb repulsion, and two types of phonon are coupled to the electronic system: intramolecular and longitudinal, intercell vibrations. The special case of half an electron per cell is considered. The model is solved in the Hartree–Fock approximation by assuming a possible symmetry break of period two. The solution is obtained for all temperatures. We construct a phase diagram with respect to temperature and the system parameters. Three types of low temperature ordered phase appear: bond ordered waves (BOW), charge ordered waves (COW) and an intermediate phase, across which the transition BOW → COW is continuous. This phase corresponds to a ferroelectric state (F). As temperature is increased from zero, the system undergoes different phase transitions, following a particular sequence, according to its characteristic parameters. At high temperatures the system stabilises in a homogeneous (disordered) phase (H). For some parameters the sequence BOW → F → COW → H is possible. The last result is very striking, since it implies that, on increasing temperature, the symmetry of the system can decrease, as is the case for the BOW → F transition, where the inversion symmetry is lost. This special BOW → F phase transition also occurs in the non-interacting limit, where our results are exact.

1. Introduction

One-dimensional electronic systems coupled to lattice deformations have been extensively studied in the literature both experimentally and theoretically over the last two decades [1–20]. Models with different degrees of complexity have been introduced, and various types of solution have been attempted.

Three main aspects determining physical properties of these systems must be considered: the number of conduction electrons per cell, n; the importance of Coulomb repulsion compared with the bare bandwidth; and the types of electron–phonon coupling. Roughly, these coupling types may be related to local variations in the intercell distances [1–15] (and thus, to changes in the electronic transference integral) or low-energy intramolecular deformations [16–20] (associated with a local change in molecular electronic affinity).

The temperature (T) is another obvious external element to be considered in determining the stable state of the system [15, 18], although a great amount of existing literature is devoted only to the $T = 0$ K case.

0953-8984/90/163723+13$03.50

According to the Peierls [1] prediction, the lattice deformation acquires a modulation of wavevector $2k_F$ in the non-interacting limit, but with increasing intrasite Coulomb repulsion it changes continuously [13, 18] into a $4k_F$ modulation, thus giving rise to a Wigner crystal. In general, the broken-symmetry lattice period depends critically on both the electronic concentration, n, and the relative magnitudes of different Coulomb repulsions [12, 13, 18]. Locking to a simple commensurate period is also present [12, 18].

Ignoring spin degrees of freedom, these one-dimensional lattices mainly develop two types of broken symmetry: bond ordered waves (BOW) or charge ordered waves (COW). A BOW corresponds to a periodic alternance of molecular distances, and it is stabilised by a strong intermolecular phonon–electron coupling. On the other hand, a COW corresponds to an alternance in molecular electronic occupancy, and it is favoured by a strong electron–electron first-neighbour Hubbard repulsion; also an intramolecular soft mode stabilises COW.

The properties and relative stability of BOW and COW have been studied in the literature for different systems. In the case $n = 1$ some stability criteria have been obtained [11, 17]. Also the magnitude of BOW distortions has been analysed in terms of Coulomb interactions for $n = 1$ [8–10, 19], $n = \frac{1}{2}$ [14, 18], and other n-values. Intermediate values of intracell ($n = 1$ case) and first-neighbour ($n = 0.5, 1$ cases) Coulomb repulsion increase the magnitude of BOW, while a strong Coulomb interaction inhibits BOW. However, going beyond the extended Hubbard [21] model, the Coulomb repulsion always seems to inhibit BOW [10].

In the limit of infinite intracell repulsion U, the extended Hubbard–Peierls model is equivalent to a spinless electronic system [13, 16], as long as we do not focus on magnetic properties [13]. In this case, and for $n = \frac{1}{2}$, the distortion wave has period two (say, a wavevector $2k_F$ for spinless fermions, or equivalently, $4k_F$ for spin $\frac{1}{2}$). However, a long range Coulomb repulsion can lead to a period-four wave [16], and the same is true for a large but not infinite value of U [13].

In this case of spinless electrons, and in a nearly rigid lattice at low temperature, a COW with period two is stable for $G_1 > 2t$, $G_j = 0$ and $n = \frac{1}{2}$ [14]. Here t is the electronic transference energy and G_j is the Coulomb repulsion between electrons j sites apart. For other values of n and long range Coulomb repulsion, more complicated COW are possible [11, 18, 21]. However, as lattice deformations are included, BOW are also possible. Working on this case of spinless electrons in finite rings at $T = 0$, Gagliano *et al* [14] have obtained a BOW/COW stability map in terms of G_1 and a parameter that accounts for intercell deformations; they do not include on-cell (molecular) deformations. Their map shows an intermediate region where COW and BOW coexist; but the boundary of this intermediate zone is not sharply established. Kivelson [4] has also obtained coexistence between BOW and COW in a non-interacting Peierls model with on-cell and intercell displacements. He also worked at $T = 0$. This BOW–COW coexistence implies a breakdown of crystal inversion symmetry, and thus, the appearance of static electric dipoles that give rise to a ferroelectric phase (hereafter denoted by F).

In this work we study a spinless one-dimensional fermion gas, $n = \frac{1}{2}$, for which first- and second-neighbour repulsions are included, and also intramolecular and intermolecular phonon–fermion interactions are considered.

The calculations are for arbitrary temperatures. The Hartree–Fock (HF) approximation is used, including its exchange contribution, which, in this work plays an important role.

We make the assumption of $2k_F$ (period-two) distortions, which is appropriate for moderate second-neighbour interaction [16].

We obtain the phase diagram in terms of the system parameters and temperature. At low temperatures there are BOW and COW stability regions, and between them, a small ferroelectric zone, which accounts for the continuous change from BOW to COW. At high temperature the disordered, homogeneous phase (H) is stable.

On increasing temperature, the H region is attained through different phase sequences, according to the parameter values that characterise the system. In particular, for some values the sequence BOW → F → COW → H occurs as temperature is increased. The last case is remarkable, since it implies a symmetry decrease as temperature is increased; in fact, the F phase lacks inversion symmetry. We note that this result remains valid in the non-interacting limit, where our treatment is exact.

We display the phase diagram by drawing different slices of the parameter space; the order parameters characterising each phase are also displayed.

The plan of this work is as follows: in section 2 the model is introduced and solved in the HF approximation; in section 3 the results are presented and a comparison is made with the exact solution for a small cluster; in section 4 the results are discussed and summarised.

2. The model

Our starting point is a spinless electron system, with half an electron per crystalline cell; its dynamics is described by a generalised Hubbard–Peierls model with electronic hopping between neighbouring sites, and Coulomb repulsion between first and second neighbours. We also introduce couplings between electrons and two types of vibrational degrees of freedom: intra- and intercell deformations. The Hamiltonian has the form

$$\check{H} = \sum_l [-(t - gu_l)(c_l^\dagger c_{l+1} + c_{l+1}^\dagger c_l) + n_l(G_1 , n_{l+1} + G_2 n_{l+2}) + \lambda v_l n_l + \tfrac{1}{2}(Ku_l^2 + Qv_l^2)] \tag{1}$$

where $c_l^\dagger$ creates a spinless fermion in site l, $n_l = c_l^\dagger c_l$ is the number of particles in l, G_1 and G_2 are the Coulomb repulsions between first and second neighbours respectively, $u_{l+1} - u_l$ and v_l represent intermolecular and intramolecular distortions, and λ, g are their respective couplings to the electrons. The last term in (1) is the potential energy of the vibrations.

According to [19], the zero-point quantum fluctuations are small in many actual systems. So, we disregard the ionic kinetic energy in (1) (adiabatic approximation), and thus the coordinates u_l, v_l behave as classical parameters, which adopt the values that minimise the Helmholtz free energy $F[u_l, v_l]$. Applying the Hellmann–Feynman theorem, the equilibrium values for these variables can be evaluated:

$$\partial F/\partial u_l = 0 = 2g\langle\langle c_l^\dagger c_l\rangle\rangle + ku_l \tag{2}$$

$$\partial F/\partial v_l = 0 = \lambda\langle\langle n_l\rangle\rangle + Qv_l \tag{3}$$

where $\langle\langle \ldots \rangle\rangle$ represents the thermal quantum averaging.

Now, in order to obtain a diagonalisable bilinear Hamiltonian we apply the Hartree–Fock (HF) approximation to the Coulomb electron–electron interaction:

$$\sum_l n_l n_{l+h} \longrightarrow \sum_l n_l(\langle\langle n_{l+h}\rangle\rangle + \langle\langle n_{l-h}\rangle\rangle) - c_l^\dagger c_{l+h}\langle\langle c_{l+h}^\dagger c_l\rangle\rangle - c_{l+h}^\dagger c_l\langle\langle c_l^\dagger c_{l+h}\rangle\rangle. \tag{4}$$

At this point we introduce the hypothesis of a period-two distortion, motivated by the electronic density $n = \frac{1}{2}$ and the condition $G_2 < \frac{1}{2}G_1$ [16]. We do that by postulating the averages

$$\langle\langle c_l^\dagger c_{l+j}\rangle\rangle = \tau_j + (-1)^l\Delta_j \qquad j = 1,2 \tag{5}$$

$$\langle\langle \check{n}_l\rangle\rangle = \tfrac{1}{2} + (-1)^l\Gamma. \tag{6}$$

Here Γ measures the fluctuation of charge in site l. Using relations (2) and (3) it is seen that Δ measures the fluctuation of molecular distance along the chain, and Γ is proportional to fluctuations in the intramolecular degree of freedom v_l. We remark that $\Gamma \leq \frac{1}{2}$ and $\Delta \leq \frac{1}{4}$. The case $\Gamma = \frac{1}{2}$ represents a saturated COW, with charges 0 and 1 alternating. For $\Delta_1 = \frac{1}{4}$ it holds that $\tau_1 = \frac{1}{4}$ and then the electronic delocalisation $\langle\langle c_l^\dagger c_{l+1}\rangle\rangle$ alternates between 0 and $\frac{1}{2}$; thus, in this limit the system breaks into $N/2$ molecular dimers, without electronic exchange between different dimers.

Substituting (2)–(6) in relation (1), we obtain the effective Hamiltonian

$$\check{H}_{\text{eff}} = -\sum_l \{[W + (-1)^l G\Delta_1]c_l^\dagger c_{l+1} + G_2[\tau_2 + (-1)^l\Delta_2]c_l^\dagger c_{l+2} + \text{HC}\} - V\Gamma\sum_l (-1)^l\check{n}_l. \tag{7}$$

Here HC symbolises the Hermitian conjugated operator, and

$$\begin{aligned} G &= G_1 + \tfrac{1}{2}D_{\text{B}} \\ V &= 2(G_1 - G_2) + D_{\text{C}} = 2G + D \\ W &= t + G\tau_1 \end{aligned} \tag{8}$$

with

$$D_{\text{C}} = \lambda^2/Q \qquad D_{\text{B}} = 4g^2/K \tag{9}$$

and

$$D = D_{\text{C}} - D_{\text{B}} - 2G. \tag{10}$$

We note that the effective electronic transference, W, has been increased in relation to the 'bare' transference t by an exchange HF contribution.

The Hamiltonian (7) is easily diagonalised in the Bloch representation, because it only mixes momenta k and $k + \pi$. In the new reduced Brillouin zone scheme, $-\pi/2 \leq k \leq \pi/2$, the eigenvalues are

$$W_k^{\pm} = -2G_2\tau_2\cos(2k) \pm \{4W^2\cos^2 k + 4G^2\Delta_1^2\sin^2 k + [V\Gamma + 2G_2\Delta_2\cos(2k)]^2\}^{1/2}. \tag{11}$$

Thus, in general, a gap may be present between the lower (filled) and upper (empty) bands, stabilising the distorted phase at low temperatures. In the case $\tau_2 = 0$ the particle–hole symmetry is preserved [4,22], $W_k^- = -W_k^+$ and the energy gap existence is assured.

The Helmholtz free energy in the HF approximation is evaluated in the standard way, giving

$$F = -\frac{k_B T}{\pi N} \sum_k \sum_{\xi=\pm} \log\{1 + \exp[-(W_k^\xi - \mu)/k_B T]\} + G(\tau_1^2 + \Delta_1^2) + G_2(\tau_2^2 + \Delta_2^2) + \tfrac{1}{2} V \Gamma^2 \tag{12}$$

where μ is the chemical potential and the sum runs from $-\pi/2$ to $\pi/2$.

The self-consistency equation for the averages (5) and (6) is obtained by minimising F with respect to τ_j, Δ_j and Γ. In particular, one finds

$$\tau_2 = \frac{k_B T}{\pi N} \sum_k \cos(2k) \left[f(W_k^+) + f(W_k^-) \right] \tag{13}$$

where $f(\xi) = 1/\{1 + \exp[(\xi - \mu)/k_B T]\}$ is the Fermi distribution.

However, if electron–hole symmetry holds, in this special case where $n = \frac{1}{2}$, it implies that $\mu = 0$, and so $f(W_k^-) = 1 - f(W_k^+)$ (the number of k-electrons in the lower band coincide with the number of k-holes in the upper band). By introducing this relation in (13), we conclude $\tau_2 = 0$, which, in turn, implies the electron–hole symmetry. Thus, the $\tau_2 = 0$ hypothesis is self-consistent, and we shall choose this solution in our case, $G_2 < \frac{1}{2} G_1$, because the effect of a non-vanishing τ_2 is to reduce (and eventually close) the energy gap between bands W_k^- and W_k^+, see (11); the latter points to the destabilisation of an ordered solution [22], and to an increase in the Helmholtz free energy. Moreover, we have verified that a spontaneous breakdown of electron–hole symmetry is only stable for $G_2 < \frac{1}{2} G_1$ in the isotropic, period-one solution. Incidentally, we note that the same restriction holds for the stability of a period-four COW [16].

The other averages, obtained by minimising F, obey the self-consistency relations

$$\Gamma = \frac{1}{\pi} \int_0^{\pi/2} \mathrm{d}k \, \frac{1}{W_k} [V\Gamma + 2G_2 \Delta_2 \cos(2k)] \tanh\left(\frac{W_k}{2T}\right) \tag{14}$$

$$\Delta_1 = \frac{1}{\pi} \int_0^{\pi/2} \mathrm{d}k \, \frac{1}{W_k} [2G\Delta_1 \sin^2(k)] \tanh\left(\frac{W_k}{2T}\right) \tag{15}$$

$$\tau = \frac{1}{\pi} \int_0^{\pi/2} \mathrm{d}k \, \frac{1}{W_k} [2W \cos^2(k)] \tanh\left(\frac{W_k}{2T}\right) \tag{16}$$

$$\Delta_2 = \frac{1}{\pi} \int_0^{\pi/2} \mathrm{d}k \, \frac{\cos(2k)}{W_k} [V\Gamma + 2G_2 \Delta_2 \cos(2k)] \tanh\left(\frac{W_k}{2T}\right) \tag{17}$$

where $W_k = W_k^+$. We have numerically estimated the upper bound $\Delta_2 < 0.08$; thus, for $G_2 < \frac{1}{2} G_1$ the contribution of $G_2 \Delta_2$ to the one-particle energy W_k^ξ is negligible. Hereafter $\Delta_2 = 0$ and $\Delta_1 =: \Delta$; this is the only approximation in our calculations apart from the HF approximation. It only remains to solve the set of equations (14)–(16). When a pure BOW ($\Gamma = 0$), or COW ($\Delta = 0$) phase is stable, the set of equations reduce to two.

In the F phase ($\Gamma \neq 0, \Delta \neq 0$) a simple relation for τ holds:

$$\tau = 2W\left(\frac{1}{V} - \frac{1}{2G}\right) \tag{18}$$

as is easily verified from (14)–(16). Thus, in this case the number of equations also reduces to two.

At this point we note that the seven initial parameters have been reduced to three in the HF approximation: t, D and G. The first one is related to the electronic delocalisation, although it appears renormalised by the exchange HF contribution, $t \to W = t + G\tau_1$. This 'band broadening' (due mainly to first-neighbour repulsion G_1) seems not to be a spurious effect, as the present results and [23] suggest. We shall take $t = 1$ as a scaling choice.

The parameter $D = D_C - D_B - 2G_2$ is important in detecting the stable phase at low temperature; if the intermolecular Hooke constant K is very small, then $D_B \to -\infty$, $D \to -\infty$ and a BOW is stable. The same is also true for a large value of G_2, as second-neighbour repulsion prevents a period-two COW from stabilising. If the intramolecular elastic constant is very soft instead, $Q \to 0$, $D_C \to \infty$ and $D \to +\infty$, thus stabilising a COW. Also, a large value of G stabilises a COW.

3. Results

We shall analyse the most stable self-consistent solution for the order parameters Γ, Δ and τ across the bidimensional space parameter of the system (G, D), and for different temperatures ($t = 1$ is our energy unit).

We shall consider the four types of solution previously introduced: COW ($\Delta = 0$), BOW ($\Gamma = 0$), F ($\Gamma \neq 0$, $\Delta \neq 0$) and homogeneous, H ($\Gamma = \Delta = 0$); and analyse their relative stability in parameter space. We shall also evaluate the order parameters, Γ and Δ, in each region. The numerical analysis of (14)–(16) leads us to the results outlined below.

3.1. The phase diagram

In the following we describe the regions of the three-dimensional parameter space G–D–T where the different phases of our system, BOW, F, COW and H, are stable.

3.1.1. The $T = 0$ case. At $T = 0$ the COW is stable for $D > 0$ and arbitrary values of $G > 0$ (G is always positive as can be inferred from (8)).

For fixed G and decreasing D, we have a transition to a ferroelectric state at $D = D_1(G)$, and a second transition to a bond wave at $D = D_2(G)$. In figure 1 these two zone boundaries are depicted as full curves. In the limit $G \gg 1$, we get $D_1(G) \sim -G$, and $D_1(G) - D_2(G) \sim 0.02G$. For small G-values, the ferroelectric zone is very narrow, $[D_1(G) - D_2(G)]/G \ll 0.02$.

3.1.2. Temperature dependence of the phase boundaries. In order to display the temperature dependence of the phase boundaries, we intersect the parameter space with D–T planes for $G = 3.5$ (figure 2(*a*)) and $G = 41$ (figure 2(*b*)), and draw on these planes the different stable phases. Obviously, in both parts of the figure the upper zone represents the homogeneous phase, while the three lower zones represent, from left to

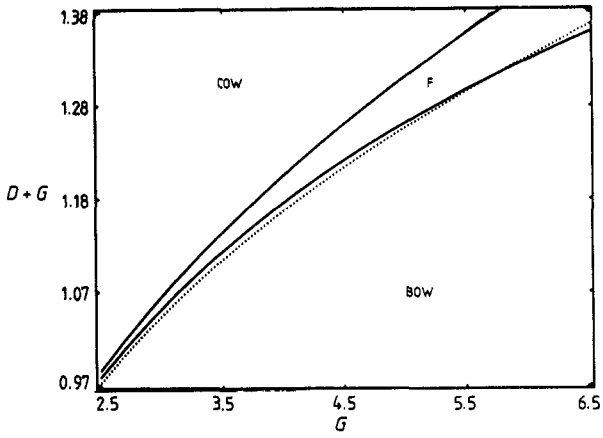

Figure 1. A projection of the phase diagram in the (G, D) plane. For magnification purposes the axes give G and $G + D$. The BOW, ferroelectric (F) and COW phases are indicated. The full curves are the phase boundaries at $T = 0$, while the dotted curve corresponds to the condition that critical temperatures for BOW and COW coincide (see text).

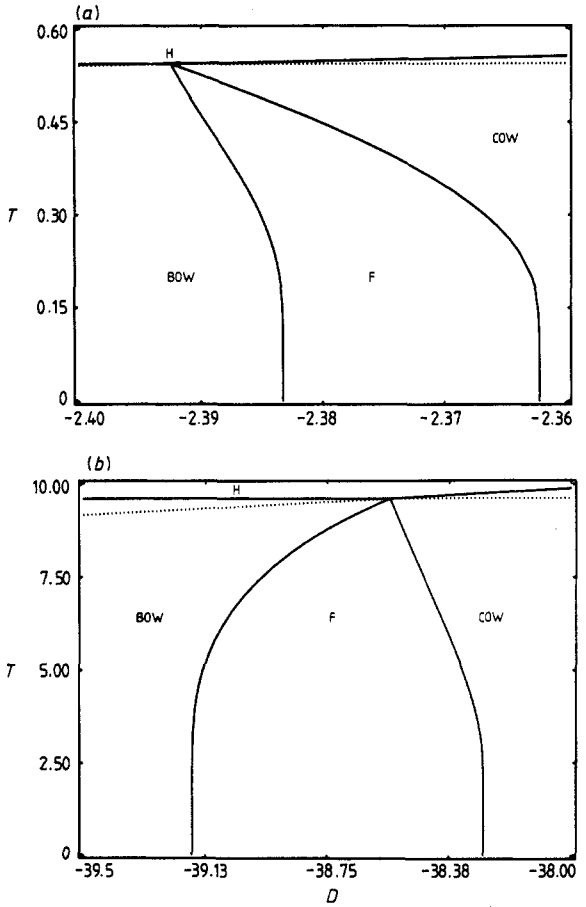

Figure 2. Slices of the phase diagram with (D, T) planes. The homogeneous (H), BOW, ferroelectric (F) and COW phases are indicated. The full (dotted) curves represent the stable (metastable) phase boundaries. (*a*) $G = 3.5$; (*b*) $G = 41$.

right, the BOW, F and COW phases respectively. The homogeneous zone is separated from the BOW and COW zones by the critical temperature curves, $T_B(G)$ and $T_C(G, D)$ respectively, the first appearing as a horizontal line in the diagrams of figure 2. These critical temperature curves are continued into dotted traces, indicating the boundaries

between the homogeneous and metastable ordered phases, the latter with lower T_C than the stable phase.

We also see from figures 2(*a*) and 2(*b*) that ferroelectric zone becomes narrower as T increases, and it reduces to just a point, $(D_F(G), T_F(G))$, at the critical temperature where the two order parameters vanish, $\Gamma = \Delta = 0$.

At that point (the 'vertex' of the F phase), the BOW and COW critical temperature curves intersect, $T_C[G, D_F(G)] = T_B(G) \equiv T_F(G)$.

In the case $G = 3.5$, the ferroelectric zone has a horn shape, with its vertex being to the left of the BOW–F boundary. In the case $G = 41$ the vertex lies between the BOW–F and F–COW boundaries.

In order to obtain more general insight, in figure 1 the 'ferroelectric vertex' is projected onto the G–D plane, $D_F(G)$, as the dotted curve therein. It should be stressed that the ferroelectric vertex lies to the left of the BOW–F, $T = 0$ boundary if $G < 5.75$, and it lies between the BOW–F and F–COW boundaries for $G > 5.75$. In this way, for $G < 5.75$ and a suitable D-value, the following sequence of phase transitions can take place: BOW → F → COW → H, as can be seen from figure 2(*a*). This is a surprising result, as the F phase (which lacks inversion symmetry) has lower symmetry than the BOW phase.

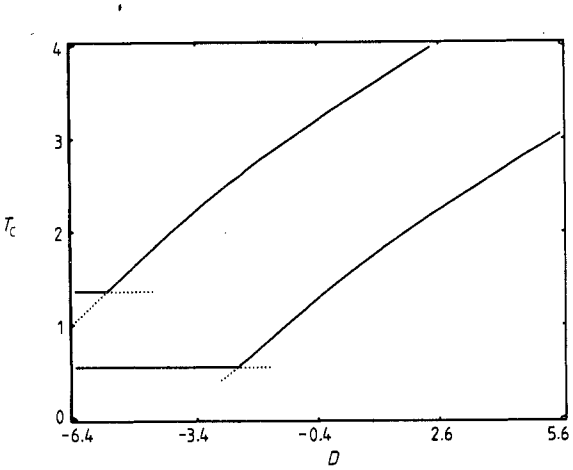

Figure 3. Critical temperature versus D for $G = 7$ (upper curve) and $G = 3.5$ (lower curve). The right (left) side corresponds to the COW → H (BOW → H) transition.

3.1.3. Critical temperature. In figure 3 we represent the critical temperature versus D for $G = 3.5$ and $G = 7.0$ (lower and upper curves respectively); the left hand side of the figure corresponds to the BOW → H transition (horizontal curve), while the right hand side corresponds to the COW → H transition.

We note that, as other properties of the BOW, its critical temperature does not depend on D.

3.2. Order parameters

In figure 4(*a*) we show the dependence of the BOW parameters τ and Δ on G; we choose $T = 0$ there. It can be seen that $\tau \sim \frac{1}{4} + \frac{1}{2G}$; $\Delta \sim \frac{1}{4} - \frac{1}{2G}$ for $G \to \infty$; in this way the electronic transference between two dimers, $\tau_{l,l+1} = \tau - \Delta$, becomes negligible in this case. The latter limit is attained for a very narrow conduction band, $G \gg t$, and

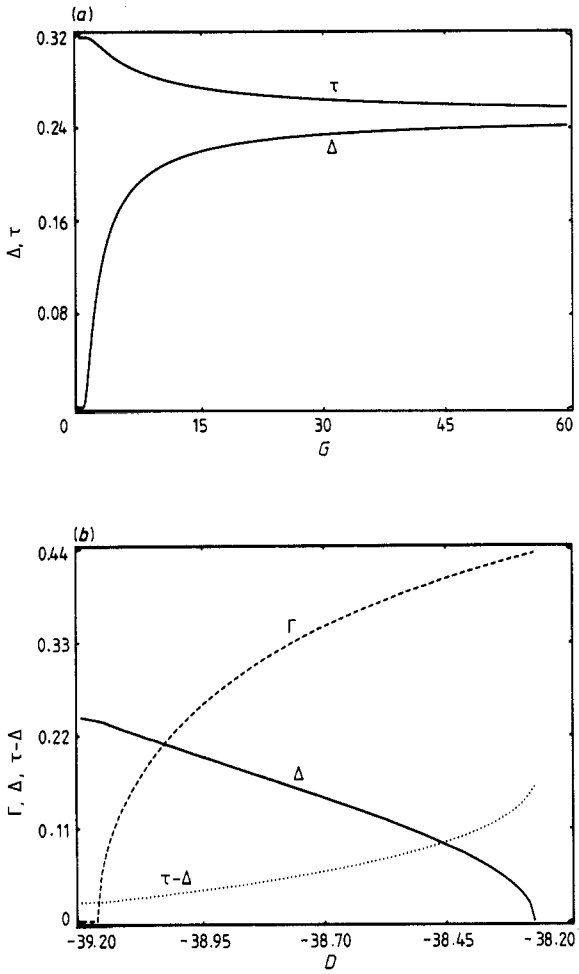

Figure 4. Order parameters at $T = 0$. (*a*) τ and Δ versus G for the BOW phase. (*b*) Δ (full curve), Γ (broken curve) and the electronic transference between dimers $\tau - \Delta$ (dotted curve) versus D for $G = 41$; here the system crosses from BOW (left) to COW (right) through the ferroelectric phase.

for a small Hooke constant under lattice contractions, $K \to 0$. As is quite natural on physical grounds, the last condition assures the stability of the BOW, say as $D \to -\infty$, and thus $D < D_2(G) \sim -G$ (see (8)–(10)).

In figure 4(*b*) the parameters Γ, Δ and $\tau - \Delta$ are displayed for $T = 0$, $G = 41$ and D crossing the transition region BOW → F → COW. There it is apparent that the system changes continuously from a nearly dimerised BOW (left), with $\tau - \Delta \sim 0$, to an almost saturated COW (right), for which $\Gamma \sim \frac{1}{2}$. In the COW phase, Γ increases with D and G; if G or D goes to infinity, $\Gamma \to \frac{1}{2}$.

In figure 5 the temperature dependence of the order parameters Δ (full curve) and Γ (broken curve) is depicted. There $G = 3.5$ and $D = -2.388$; in accordance with figure 2(*a*), the system moves over the four phases as T is increased. In fact, for $0 < T < 0.4024$ the system is a BOW, $\Delta \neq 0$, $\Gamma = 0$. For $0.402 < T < 0.494$ the two order parameters coexist, $\Delta \neq 0$, $\Gamma \neq 0$, in a ferroelectric phase. At $T = 0.494$, Δ vanishes and Γ shows a kink; from then on, Γ decreases continuously, reaching the COW → H transition at $T = 0.546$.

It holds that the order parameters Δ and Γ vanish according to the law, $(T_C - T)^{0.5}$,

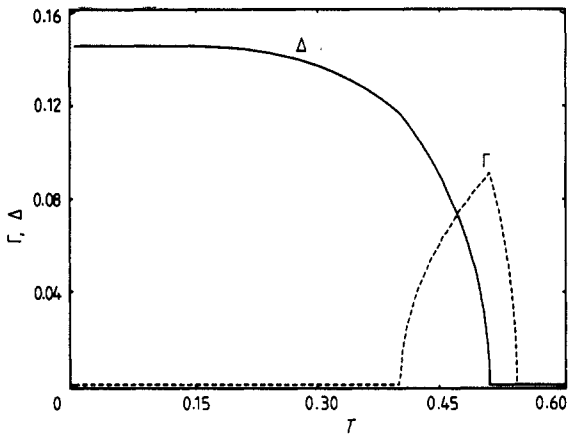

Figure 5. The order parameters versus temperature for $G = 3.5$ and $D = -2.388$; the system follows the sequence of phase transitions BOW → F → COW → H as T is increased.

thus showing a typical critical exponent of the Hartree–Fock approximation.

3.3. Comparison with some exact results

In spite of its simplicity, the HF approximation has severe limitations, especially for studying excited states [24]. Nevertheless, HF is currently used on these one-dimensional systems [5, 6, 17]. In order to analyse its accuracy, we have studied a four-atom, two-spinless-electron system described by our Hamiltonian. We have solved it exactly and in the HF approximation, since in this way a comparison of both results is a good measure of the failures of HF, as the finite size effects influence both solutions at the same level. The exact results for this four-atom cluster depend on D_C and D_B (see (10)) separately, in contrast to the HF results.

Figure 6(*a*) shows the HF and exact results for Γ in the COW phase; there $G = 3$, $D_B = 0$ and $0 \leq D_C \leq 2$. The heavy curve represents HF results for $0 \leq T \leq 0.9$, as a variation of T in this range leads to a change in Γ of less than 1%. This curve coincides precisely with the $T = 0$ exact result for Γ. As T is increased, the exact COW solution is stable only up to a certain critical value of D_C; for example, at $T = 0.5$ (broken curve) the COW, $\Gamma \neq 0$, solution exists if $D_C > 0.75$, while for $T = 0.9$ (dotted curve), $\Gamma \neq 0$ for $D_C > 1.31$.

In this way, the finite size exact results suggest that the temperature breaks down the ordered phases faster than predicted by HF analysis. It should be stressed that the exact results for the four-atom system always yield a critical temperature $T_C < D_C$ for the COW → H transition. This result strongly contrasts with the HF solution for both finite and infinite systems. However, the last results are not surprising, since it is well known that HF solutions tend to maintain the ordered phases beyond their physical range of stability.

In figure 6(*b*) the phase diagram of the four-atom system is shown in the (D_C, D_B) plane for $G_1 - G_2 = 0$.

The full curves indicate the COW–F (right) and F–BOW (left) boundaries. As in figure 1, the dotted curve represents the condition that the critical temperature of COW and BOW phases coincide.

In figure 6(*b*) we see that the dotted curve lies in the ferroelectric zone for $D_C < 2.3$ and it crosses the COW zone for $D_C > 2.3$. This non-interacting, $N = 4$, case may

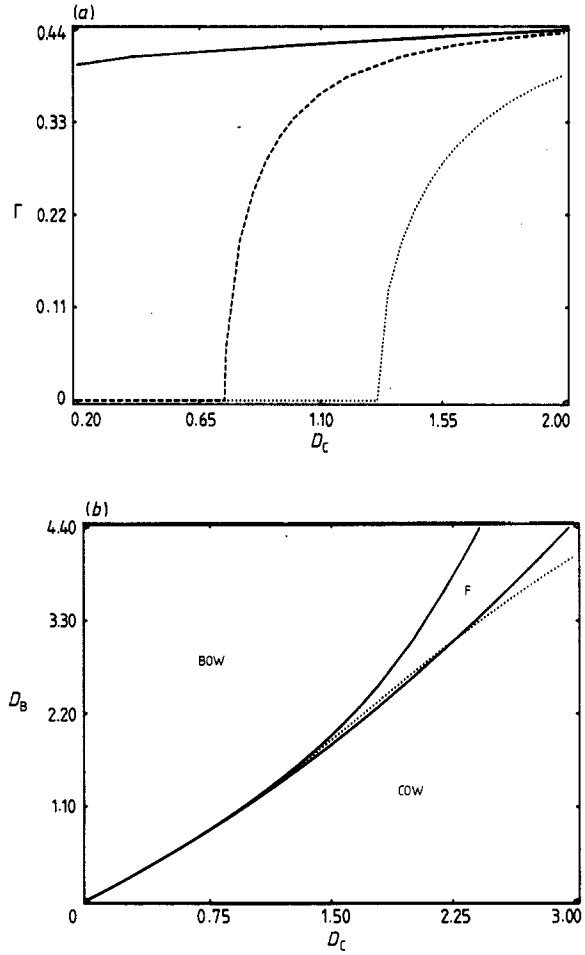

Figure 6. Exact results for a four-site system. (*a*) The order parameter Γ in the COW phase. Here $D_B = 0$, $G = 3.5$ and $T = 0$ (full curve), $T = 0.5$ (broken curve) and $T = 0.9$ (dotted curve). Also, the full curve corresponds (within the figure resolution) to HF results for these three temperature values. (*b*) A projection of phase diagram in the (D_C, D_B) plane for $G_2 - G_1 = 0$. The phases and curves are as given in figure 1. For convenience, the distance between the COW–F boundary and the other curves is magnified by a factor of 10 in the vertical direction, the first curve remaining unchanged.

be compared directly with the HF, $N = \infty$, results, as these are also exact in the $G_1 = G_2 = 0$, $G = \frac{1}{2}D_B$ case. We see that the effect of the finite size is to push the $T_B = T_C$ dotted curve into the COW phase. The results of figure 6(*b*), as other calculations for $G_1 \neq G_2$, show that the sequence of phases COW → F → BOW → H with increasing temperature is possible for the four-site ring, especially for $G > t$, in contrast with the $N = \infty$ results. However, as the $N = \infty$ HF calculations are not reliable for large values of G; we cannot assert whether the COW → F transition is a spurious finite size effect (as suggested by the $G = 0$ results), or if it remains in the $N = \infty$ limit. It is important to note that, due to degeneracy of the ground state [14], the $N = 4$ results are not very suitable for extrapolation to macroscopic systems. Calculations with larger finite size systems are needed to elucidate this point.

4. Summary and discussion

We now list the main results and limitations of the present work.

(i) There is a great richness of phase transitions as the system parameters and temperature are changed. We notice the existence of a breakdown of symmetry with *increasing temperature*, in the sequence of phase transitions BOW → F → COW → H (see figures 2(*a*) and 5). Parametric phase transitions are also apparent; these transitions may be found experimentally by choosing a particular system near the stability boundary, and then applying pressure in order to change the system parameters [4], in particular the hopping integral t. Obviously, our work suggests an easier experimental method for searching for these transitions—say a simple variation of temperature.

Although it is not usual to find a symmetry breakdown on increasing temperature, this phenomenon is not new [25]. The re-entrant superconductivity [26] is a remarkable example of an ordered phase attained by an increase of temperature.

It is important to note that a suitable treatment of a ferroelectric phase must include the effect of molecular polarisability due to a dipole electric field. So, for an actual system, the latter must increase the stability region of ferroelectricity obtained in our calculations, thus facilitating the search for it in actual systems.

(ii) The validity of the conclusion in point (i) is ensured in the non-interacting limit, where the parameters of figures 1–5 must be interpreted as $D = D_C - D_B$ and $G = \frac{1}{2}D_B$. They also seem reliable in the weak interaction limit. For $G_1, G_2 > t$, the HF approximation departs from its range of validity. Then, it is no longer a suitable description of the system in terms of the reduced parameters D and G of (9).

(iii) Our finite size results confirm the general expectation that the HF approximation works better for systems with a gap between the ground state and the first excited states [5, 24], and for low temperatures. Although the coincidence between exact and HF results for a four-site ring in a COW state at $T = 0$ seems fortuitous, our hope is that HF is specially suitable in this phase and for low temperature, a hope which is supported by previous results [23]. In this way, the band broadening due to the HF exchange term, $t \to t + \tau G$, seems not to be a spurious effect.

(iv) It is important to introduce both, intra- and intersite lattice degrees of freedom, as the intramolecular parameter $D_C = \lambda^2/Q$ contributes in determining the phase boundaries [4]. The importance of the intrasite degrees of freedom is apparent from our reduced HF parameter $D = D_C - D_B - 2G_2$ of figures 1–5, and from our exact calculations of figure 6(*b*). This contribution must be considered in theoretical models in order to describe realistic quasi-one-dimensional systems.

Acknowledgments

We would like to acknowledge G Martínez for his help with this paper. This work was supported by FONDECYT, under Grant No 1129–88.

References

[1] Peierls R E 1955 *Quantum Theory of Solids* (Oxford: Clarendon) p 108
[2] Rice M J and Strassler S 1973 *Solid State Commun.* **13** 125
[3] Su W-P, Schrieffer J R and Heeger A J 1980 *Phys. Rev.* B **22** 2099

[4] Kivelson S 1983 *Phys. Rev.* B **28** 2653
[5] Hicks J C and Tinka Gammel J 1988 *Phys. Rev.* B **37** 6315
[6] Kivelson S and Heim D E 1982 *Phys. Rev.* B **26** 4278
[7] Hirsch J E and Grabowski M 1984 *Phys. Rev. Lett.* **52** 1713
[8] Hayden G and Mele E 1985 *Phys. Rev.* B **32** 6527
[9] Soos Z G and Hayden G W 1988 *Mol. Cryst. Liq. Cryst.* **160** 421; 1989 *Phys. Rev.* B **40** 3081
[10] Kivelson S, Su W-P, Schrieffer J R and Heeger A J 1987 *Phys. Rev. Lett.* **58** 1899
[11] Mazumdar S and Campbell D K 1985 *Phys. Rev. Lett.* **55** 2067
[12] Mazumdar S, Dixit S N and Bloch A N 1984 *Phys. Rev.* B **30** 4842
[13] Zhang S C, Kivelson S and Goldhaber A S 1987 *Phys. Rev. Lett.* **58** 2134
[14] Gagliano E R, Proetto C R and Balseiro C A 1987 *Phys. Rev.* B **36** 2257
[15] Gottlieb D and Lagos M 1989 *Phys. Rev.* B **39** 2960
[16] Emery V J and Noguera C 1988 *Phys. Rev. Lett.* **60** 631
[17] Conradson S D, Stroud M A, Zietlow M H, Swanson B I, Baeriswyl D and A R Bishop 1988 *Solid State Commun.* **65** 723
Baeriswyl D and Bishop A R 1988 *J. Phys. C: Solid State Phys.* **21** 339
[18] Hirsch J E and Scalapino D J 1983 *Phys. Rev.* B **27** 7169; 1984 *Phys. Rev.* B **29** 5554
[19] Fradkin E and Hirsch J E 1983 *Phys. Rev.* B **27** 1680
Hirsch J E 1983 *Phys. Rev. Lett.* **51** 296
[20] Schmidt W and Schreiber M 1986 *Z. Phys.* B **62** 423
Proetto C R and Falicov L M 1989 *Phys. Rev.* B **39** 7545
[21] Hubbard J 1978 *Phys. Rev.* B **17** 494
[22] Gottlieb D and Melo F 1988 *Nuovo Cimento* D **10** 1427
Marsch E, Steeb W-H and Grensing D 1977 *J. Phys. F: Met. Phys.* **7** 401
[23] Rössler J, Fernández B and Kiwi M 1981 *Phys. Rev.* B **24** 5299
[24] Ramasesha S and Soos Z G 1985 *Phys. Rev.* B **32** 5368
[25] Landau D and Lifshitz E M 1979 *Statistical Physics* (*Theoretical Physics Course 5*) (Oxford: Pergamon) p 526
[26] Shellton R N and Horng H E 1986 *Phys. Rev.* B **33** 1671